Conference on Modelling Fluid Flow (CMFF'25)
The 19th International Conference on Fluid Flow Technologies
Budapest, Hungary, August 26-August 29, 2025

A New Viscosity Formulation for Improved Turbulence Modeling in Kolmogorov Flow

Gergely Kristóf[2], Kinga Andrea Kovács[1], Tamás Kalmár-Nagy[2], Miklós Balogh[2]

[1] Corresponding Author. Department of Fluid Mechanics, Faculty of Mechanical Engineering, Budapest University of Technology and Economics, Műegyetem rkp. 3, Budapest, 1111, Hungary, Telephone: +36-1-463-2546, E-mail: kingaandrea.kovacs@edu.bme.hu
[2] Department of Fluid Mechanics, Faculty of Mechanical Engineering, Budapest University of Technology and Economics, Műegyetem rkp. 3, Budapest, 1111, Hungary, E-mail addresses: kristof.gergely@gpk.bme.hu, kalmar.nagy.tamas@gpk.bme.hu, balogh.miklos@gpk.bme.hu.

ABSTRACT

The Kolmogorov flow, a shear flow driven by a constant inhomogeneous body force in a periodic domain, has not been widely used for turbulence modeling despite its potential benefits. Commonly used Reynolds-averaged turbulence models (e.g., standard $k-\varepsilon$, RNG $k-\varepsilon$, standard $k-\omega$, $k-\omega$ SST, GEKO) give incorrect results for this flow. Similar issues arise in applications with sustained turbulence in a closed container, like pump shut-off head modeling. In the current paper a novel eddy viscosity model, the geometry-informed (GI) model, is proposed, which constrains the turbulent length scale by accounting for wall distance, even in dissipative flow regimes. The GI model is implemented in Ansys Fluent as a user-defined formula for the standard $k-\varepsilon$ model, and it is validated against Direct Numerical Simulation (DNS) and experimental data. In addition, the results are compared with the $k-\omega$ SST model. The test cases encompass channel flow, flow over a backward-facing step (BFS), and Kolmogorov flow. Results show that the GI model better predicts the near-wall peak of turbulent kinetic energy compared to $k-\omega$ SST in channel flow, and offers improved reattachment length predictions for high Reynolds number flow over a BFS. In Kolmogorov flow, the GI model produces qualitatively correct results, but with lower velocity amplitudes than DNS due to the shortcomings of the ε transport equation. Further improvements to the turbulent kinetic energy dissipation equation are planned.

Keywords: CFD, DNS, Kolmogorov flow, RANS, turbulence modeling, turbulent viscosity

NOMENCLATURE

Re	[-]	Reynolds number
Re_Δ	[-]	filter size-based Reynolds number
H	[m]	step size
P	$[m^2 \cdot s^{-3}]$	turbulent production
S	$[s^{-1}]$	shear modulus
U	$[m \cdot s^{-1}]$	x-wise velocity
U_τ	$[m \cdot s^{-1}]$	friction velocity
$\hat{f}$	$[m \cdot s^{-2}]$	force amplitude
f	$[m \cdot s^{-2}]$	driving force
k	$[m^2 \cdot s^{-2}]$	turbulent kinetic energy
t	[s]	time
y^+	[-]	dimensionless wall distance
y_w	[m]	distance from the wall
Δ	[m]	filter size
κ_1	$[m^{-1}]$	fundamental wave number
ν	$[m^2 \cdot s^{-1}]$	kinematic viscosity
ν_t	$[m^2 \cdot s^{-1}]$	turbulent viscosity
ω	$[s^{-1}]$	eddy frequency
ε	$[m^2 \cdot s^{-3}]$	turbulent dissipation

1. INTRODUCTION

The main aim of the current study is to develop better models near production-dissipation equilibrium using results from DNS models of Kolmogorov flow and channel flow. The most widely used eddy viscosity formula – Stress and Production (SP) model – was introduced by Jones and Launder [1] as an element of the model, currently known as the standard $k-\varepsilon$ turbulence model:

$$\nu_{t,\varepsilon} = C_\mu \frac{k^2}{\varepsilon}, \quad (1)$$

where k is the turbulent kinetic energy, ε is the turbulent dissipation, and $C_\mu = 0.09$ is an empiric constant.

Eq. (1) assumes a time step proportional to the k/ε ratio at all points in the flow field. However, it can be suspected that at locations where turbulent production exceeds dissipation (i.e., k increases along the trajectory of the fluid particle), the turbulent time scale relevant to eddy viscosity is determined by the large scales associated with production rather than the small scales associated with dissipation, and therefore Eq. (2) may be a reasonable alternative to Eq. (1):

$$\nu_t = C_\mu \frac{k^2}{P}, \quad (2)$$

where P is the turbulent production. The turbulent production can be determined with the following equation:

$$P = \nu_t S^2, \tag{3}$$

where S is the shear modulus of the bulk flow. Based on these equations a production-based eddy viscosity formula can be constructed as follows:

$$\nu_{t,P} = \sqrt{C_\mu}\frac{k}{S}. \tag{4}$$

Eq. (4) – first proposed by Chou [2] – seems to be consistent with Bradshaw's observation that the primary turbulent stress is proportional to the turbulent kinetic energy at the outer boundary layer. The obvious drawback of Eq. (4) is that it results in a turbulent viscosity approaching infinity, where S approaches zero. The need to combine the turbulent viscosity formulae – Eqs. (1) and (4) – was recognized by Menter [3]. In his $k-\omega$ SST model the following eddy viscosity formula was proposed:

$$\nu_{t,\mathrm{SST}} = \frac{a_1 k}{\max\left(a_1\omega, S F_2\right)}, \tag{5}$$

where $a_1 = 0.31$ is a constant, ω is the eddy frequency, and F_2 is given by (F_2 is a function that is one for boundary layer flows and zero for free shear layers):

$$F_2 = \tanh\left(\Phi_2^2\right), \tag{6}$$

where:

$$\Phi_2 = \max\left(2\frac{\sqrt{k}}{0.09\omega y_w}, \frac{500\nu}{y_w^2\omega}\right), \tag{7}$$

where y_w is the distance from the wall.

The eddy frequency can be expressed as:

$$\omega = \frac{\varepsilon}{C_\mu k}. \tag{8}$$

By substituting Eq. (8) into Eq. (5), and utilizing that $a_1 \cong \sqrt{C_\mu}$ one can obtain the following formula:

$$\nu_{t,\mathrm{SST}} = \min\left(\frac{k^2 C_\mu}{\varepsilon}, \frac{\sqrt{C_\mu}k}{S F_2}\right). \tag{9}$$

Based on Eq. (9) it can be seen that the $k-\omega$ SST model basically chooses the smaller value from Eqs. (1) and (4). A possible physical explanation is that the eddy viscosity can be considered as proportional to the turbulent kinetic energy multiplied by a time scale (k/ε or $\sqrt{C_\mu}/S$), and that the smaller time scale, which is characteristic of the faster process, dominates among the possible time scales. The model described by Eqs. (5)-(7) thus distinguishes two main regimes, production and dissipation regimes, based on time scales.

The $k-\omega$ SST model also constrains the dissipation-based formula for low (essentially less than 100) turbulent viscosity ratios using the viscosity ratio, and the production-based formula near the wall using the wall distance. The model does not use the wall distance to constrain the turbulent length scale in the dissipation regime. The $k-\omega$ SST model therefore describes the eddy viscosity as a five-variable function: $\nu_{t,\mathrm{SST}}(S, k, \omega, \nu, y_w)$.

Out of the widely used eddy viscosity models, the realizable $k-\varepsilon$ model of Shih et al. [4] assumes a C_μ value dependent on the ratio of the time scales of turbulence and the main flow, which leads to more accurate results for free jets and boundary layer separation. However, this model is not compatible with models involving rotating coordinate systems or rotating numerical grids [5]. Overall, the development of turbulent viscosity formulae has received relatively little attention in the last three decades.

2. INVESTIGATIONAL METHOD

2.1. Kolmogorov flow

The Kolmogorov flow is a flow induced by a sinusoidally varying force field in space in a periodic flow domain. The driving force can be written in the following way:

$$f = -\hat{f}\cos(\kappa_1 y), \tag{10}$$

where $\hat{f}$ is the force amplitude, and κ_1 is the wave number.

The driving force can be seen in Figure 1, where 2Δ is the side length of the cube corresponding to the simulation domain:

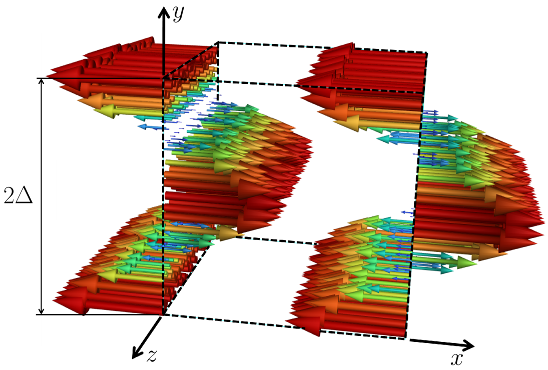

Figure 1. Spatial distribution of the driving force.

The x-wise velocity averaged in the $x-z$ planes varies with t and y as shown in Figure 2.

The Δ half side length (filter size) of the domain determines the wavenumber of the fundamental mode of the velocity field in turbulent flows, for instance, flow excited in the first mode: $\kappa_1 = \pi/\Delta$.

The reference velocity can be defined as the maximum value of the friction velocity:

$$U_\tau = \sqrt{\frac{\hat{f}}{\kappa_1}}, \tag{11}$$

and the Reynolds number being characteristic of the flow is defined in terms of the filter size:

$$\mathrm{Re}_\Delta = \frac{U_\tau \Delta}{\nu}. \tag{12}$$

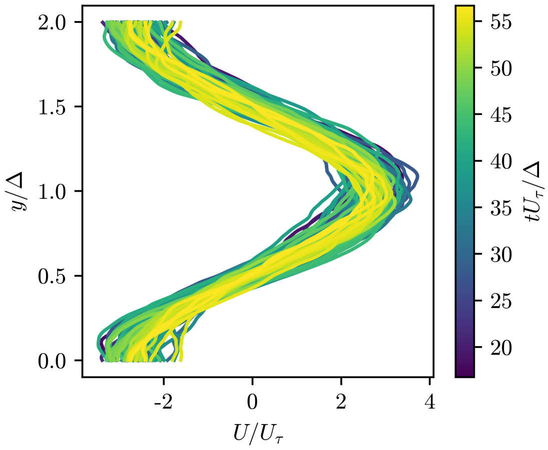

Figure 2. Dimensionless x-wise velocity profiles of the time-varying main flow. The different lines correspond to the different time steps.

Based on these equations the reference length and time are Δ and Δ/U_τ. We observed that for the quasi-stationary Kolmogorov flow, the various extensively applied Reynolds-averaged turbulence models (standard $k-\varepsilon$, RNG $k-\varepsilon$, standard $k-\omega$, $k-\omega$ SST, GEKO) lead to qualitatively incorrect results: the flow velocity amplitude decreases in time, resulting in a decrease in the spatial averages of hydraulic power, production and dissipation. On the other hand, the average value of the turbulent kinetic energy is close to the DNS results. A decreasing ε at a nearly constant k leads to an increasing turbulent viscosity, which supports the decrease in velocity amplitude at constant driving force. During this process, the turbulent length scale increases indefinitely, and this will be called herein as *turbulent inflation*.

2.2. DNS database

For the development of the eddy viscosity model, DNS model results for channel flow and Kolmogorov flow are used, which are the authors' own results in the latter case, and published data from the Johns Hopkins Turbulent Database (JHTDB) in the case of channel flow [6].

The spatially averaged characteristics of the Kolmogorov flow are strongly time-varying: Coefficient of Variation (COV) values of around 15% for S and around 20% for k are observed over the range of Reynolds numbers considered, which allows the authors to obtain data on the time variation of turbulence.

Both flow types have a layered symmetry, and therefore turbulent characteristics are derived from layer averages. The periodic lengths of the layers are $2\Delta\times2\Delta$ for Kolmogorov flow, and $8\pi\Delta_{\max}\times3\pi\Delta_{\max}$ for channel flow, where $\Delta_{\max}$ is the distance of the channel midplane from the solid wall (y-wise distance). The Reynolds averages of the physical characteristics are approximated by the two-step averaging procedure detailed below.

The value of the characteristics averaged over the x and z coordinates varies as a function of the y coordinate and time t. In the case of Kolmogorov flow, the time variation of the layer-averaged velocity results in a significant variance, which, according to the authors' interpretation, is not part of turbulence. The transient main flow forms an energy storage between the hydraulic power and the turbulent production, so there is no need for an instantaneous equilibrium between them. Although layer averaging in a periodic domain occurs in planes of infinite size, the limited period length of the domain means that the instantaneous energy spectrum of the layer averages can differ significantly from the time-averaged turbulent spectrum. Therefore, the results of models based on simplified descriptions of the turbulence state (e.g., parameters k and ε only) are subject to significant noise. The noise in the turbulent characteristics and eddy viscosity model results can be reduced by a secondary averaging. Secondary averaging can be performed t-wise or y-wise, resulting in y-direction profiles or time series. The accuracy of the different eddy viscosity models can thus be tested in either spatial or temporal projection, which is an advantage for model fitting compared to classical time-averaged methods. In the case of channel flow, only time-averaged y-dependent characteristics were determined because the large size of the model domain meant that the layer averages did not show significant temporal variation.

2.3. The method of model fitting

In the case of isotropic turbulence, the maximum wavelength of turbulent structures corresponds to the height of the model domain, which is 2Δ for Kolmogorov flow, and $2\Delta_{\max}$ for channel flow. For Kolmogorov flow, the filter size Δ is independent of the y coordinate. For channel flow, the turbulent length scale is proportional to the wall distance y_w, which is $\Delta_{\max}$ in the median plane of the channel, so the filter size Δ for channel flow is taken to be equal to the wall distance, i.e., $y_w = \Delta$. By generalizing the notion of filter size, the optimal eddy viscosity model can be searched for in a wall bounded domain, and in a periodic domain open in the y direction as a function of the same physical parameters. Thus, a common platform can be used to fit the model parameters, and a common optimum can be found for both wall boundary layer and free shear flow. From this it follows that the filter size can be determined in the case of more complex geometries as well.

3. DISCUSSION OF THE RESULTS

3.1. Geometry-informed (GI) model

In order to control the turbulent inflation in Kolmogorov flow, it is useful to consider the geometric constraints in the dissipation regime, and therefore the optimal eddy viscosity model is sought in the

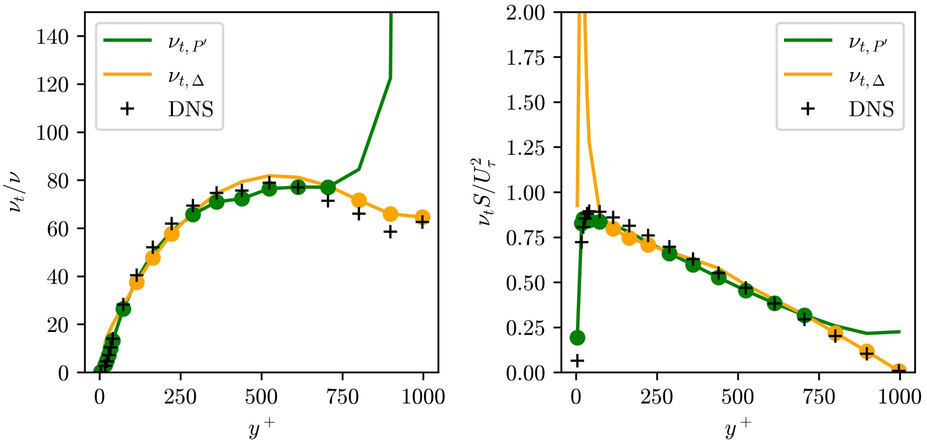

Figure 3. Comparison of dimensionless eddy viscosity (left) and turbulent shear stress (right) obtained from the proposed GI model with the DNS reference data for channel flow. The GI model uses the minimum of formulae $\nu_{t,P'}$ (green), and $\nu_{t,\Delta}$ (orange) indicated by the circular symbols.

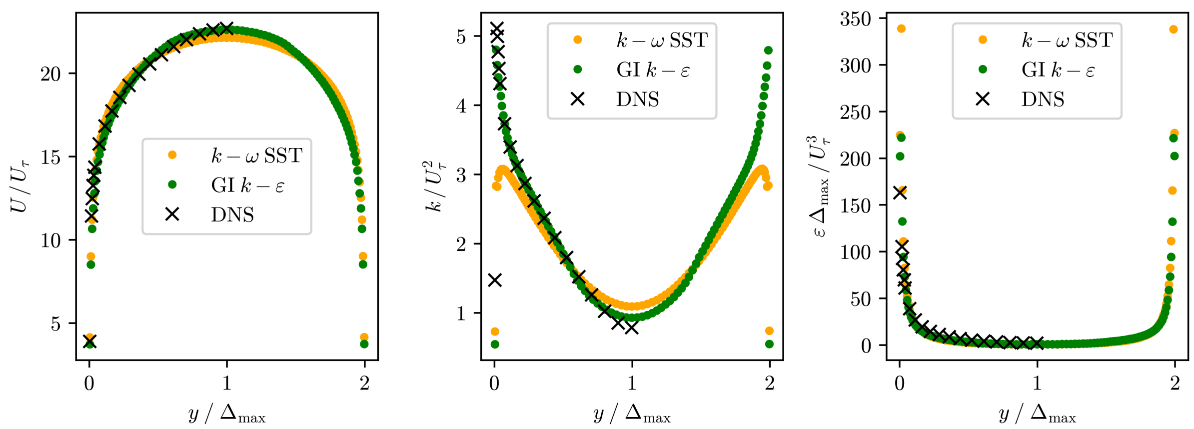

Figure 4. Streamwise velocity component (left), turbulent kinetic energy (middle), and turbulent kinetic energy dissipation (right) profiles in steady-state channel flow.

following form:

$$\nu_{t,\mathrm{GI}} = \min(\nu_{t,P'}, \nu_{t,\Delta}), \tag{13}$$

where:

$$\nu_{t,P'} = C_1 \frac{k}{S} \frac{1}{1 + e^{\left(-C_3 \frac{\sqrt{k}\Delta}{\nu}\right)}}, \tag{14}$$

and:

$$\nu_{t,\Delta} = C_2 \frac{k^{5/4}\sqrt{\Delta}}{\sqrt{\varepsilon}}. \tag{15}$$

The model constants were optimized based on channel flow, and quasi-stationary and decaying Kolmogorov flows. The minimum fitting error was observed for parameters $C_1 = 0.2535$, $C_2 = 0.1118$, and $C_3 = 0.0147$.

Figure 3 shows the GI model in equilibrium channel flow as a function of the y^+ dimensionless wall distance. It can be seen that only the production-based formula gives realistic results in the near-wall buffer layer and only the filter-based formula gives realistic results in the centerline of the channel (near $y^+ = 1000$). In the large part of the wall boundary layer the two formulae give nearly identical results. The GI model, which selects the smaller value out of the two alternative formulae, shows good agreement with the DNS reference data over the entire profile.

3.2. Implementation of the GI model

The in-situ testing of the GI model was performed in the ANSYS Fluent 2023 R1 software, using the standard $k-\varepsilon$ model. The model was implemented as a user-defined function (UDF). The eddy viscosity formula of the standard $k-\varepsilon$ turbulence model was replaced by the GI model, and the model constant value of $C_{1\varepsilon}$ was changed from the standard 1.44 to 1.55 to better fit the boundary layer flow. In other aspects, the standard model parameters were used,

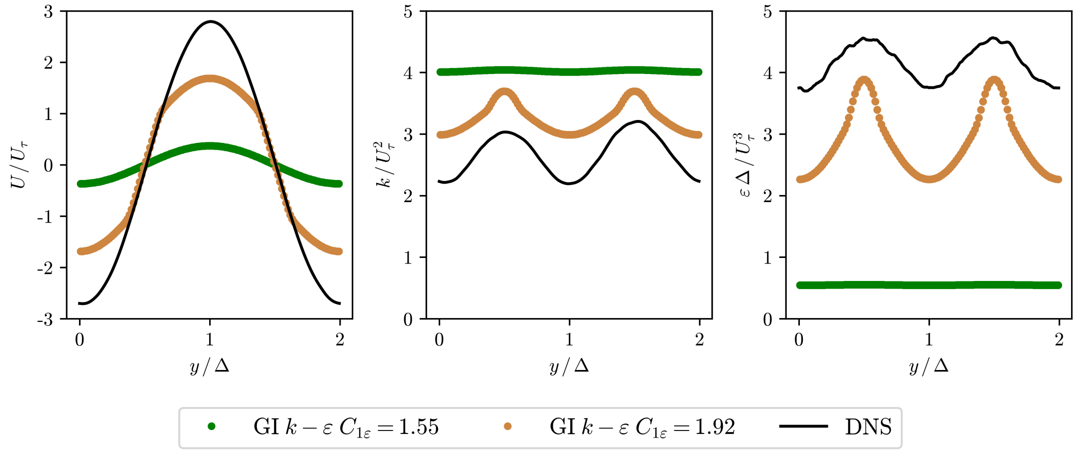

Figure 5. Streamwise velocity component (left), turbulent kinetic energy (middle), and turbulent kinetic energy dissipation (right) profiles in Kolmogorov flow.

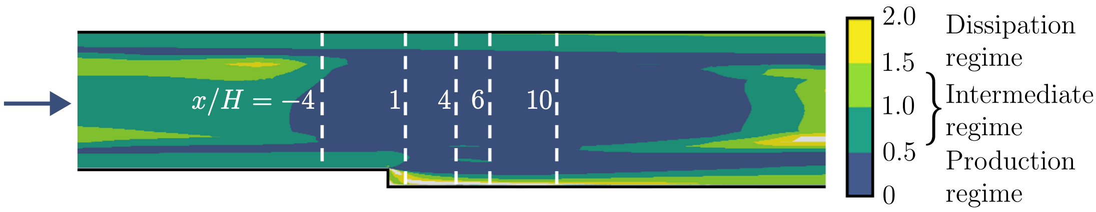

Figure 6. The value of the $\nu_{t,P'}/\nu_{t,\Delta}$ ratio calculated with the GI $k-\varepsilon$ model in the flow above a BFS. Dashed line: position of the tested profiles, and H denotes the step size.

i.e., $C_{2\varepsilon} = 1.92$, and the turbulent Prandtl coefficients of $\sigma_k = 1$, and $\sigma_\varepsilon = 1.3$ were utilized. Therefore, the constructed model is referred to as the GI $k-\varepsilon$ model herein.

3.3. Validation of the GI $k-\varepsilon$ model

Thanks to the good fit of the GI $k-\varepsilon$ eddy viscosity formula, the new turbulence model can be integrated in the turbulent boundary layer without the use of a wall function, and in addition, it can be used with a wall function if the y^+ value necessitates it.

In the case of channel flow, the mesh consisted of 1040 quadrilateral elements, with refined mesh near the wall, and a wall resolution of $y^+ = 4.3$. Periodic boundary conditions were set for the inlet, and the outlet boundaries, and the boundaries in the y-direction were specified as stationary walls. Coupled pressure-velocity coupling was used, and the following spatial discretization schemes were applied: second order for pressure, second order upwind for momentum, first order upwind for turbulent kinetic energy, and first order upwind for turbulent dissipation rate. Figure 4 shows the simulation results for the channel flow corresponding to the JHTDB test case ($\mathrm{Re} = 40\,000, \mathrm{Re}_\Delta = 1000$). It can be seen that for steady-state channel flow, the GI $k-\varepsilon$ model provides more accurate results for the near-wall peak value of the turbulent kinetic energy than the $k-\omega$ SST model.

In the case of Kolmogorov flow, the mesh consisted of 512 hexahedral elements, and periodic boundary conditions were applied. The body force was applied as an x momentum source term. The applied numerical schemes were the same as in the case of the channel flow. Figure 5 shows the simulation results of the $\mathrm{Re}_\Delta = 997$ quasi-stationary Kolmogorov flow which was excited in the first mode. The turbulent inflation observed for the known Reynolds averaged models (these could not even be fitted into Fig. 5) did not occur for the GI $k-\varepsilon$ model, so the model leads to a qualitatively different result: a convergent solution satisfying the turbulent energy balance and the discrete base equations is obtained. The model results show a high sensitivity to the value of the parameter $C_{1\varepsilon}$. With an optimal $C_{1\varepsilon} = 1.55$ setting for the channel flow, the Kolmogorov flow yields a velocity amplitude one order of magnitude lower than the DNS reference data. Based on the analysis of the DNS data, it was observed that the transport equation for dissipation only correctly describes the Kolmogorov flow around $C_{1\varepsilon} = C_{2\varepsilon}$. For the choice of $C_{1\varepsilon}$ with the same value as $C_{2\varepsilon}$, the results of the GI $k-\varepsilon$ model are remarkably closer to the DNS reference data than with the parametrization optimized for channel flow. The adaptation of the transport equation for dissipation requires further investigation.

The results of the GI $k-\varepsilon$ model ($C_{1\varepsilon} = 1.55$, $C_{2\varepsilon} = 1.92$) were tested against measurement data [7] and against the widely used $k-\omega$ SST model

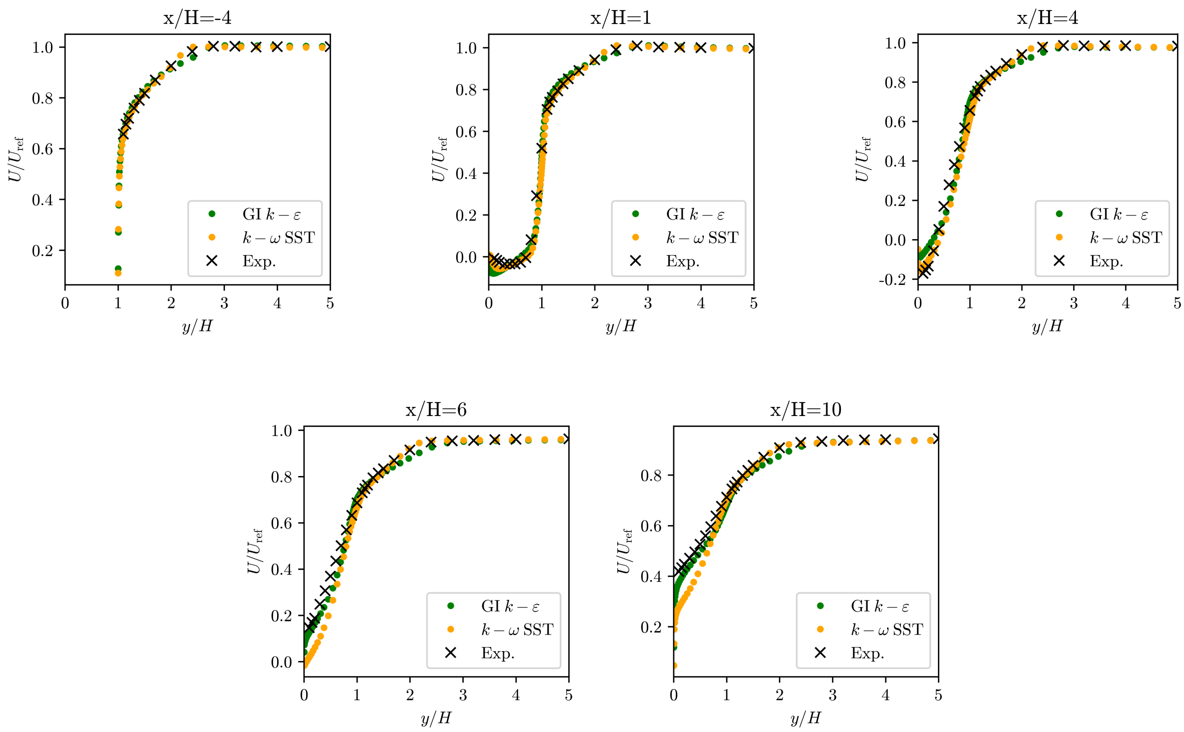

Figure 7. Normalized velocity profiles calculated from the GI $k - \varepsilon$ model (blue) compared to $k - \omega$ SST model results (orange) and measurement data (black) in flow over a BFS along different x/H profiles.

for a backward-facing step (BFS) flow. In the model domain shown in Figure 6, the fluid flows from left to right. At the edge of the step, the boundary layer separates and then reattaches to the bottom surface of the channel. The simulations were performed using a non-equidistant structured mesh with 76 180 hexahedral cells, and the grid had a $y^+ = 3$ wall resolution. For the inlet and the outlet, a velocity inlet (based on [7]) and a pressure outlet boundary condition were prescribed, respectively. For the lower and upper boundaries, wall boundary conditions were prescribed, and for the other boundaries a symmetry boundary condition was set. Coupled pressure-velocity coupling was used, and second order numerical schemes were utilized.

In Figure 6 the coloring shows the value of the $\nu_{t,P'}/\nu_{t,\Delta}$ ratio. For values less than 1 the GI $k - \varepsilon$ model applies the production-based formula ($\nu_{t,P'}$) and for values greater than 1 the filter-based formula ($\nu_{t,\Delta}$). In the intermediate (green) regions, local production and dissipation are approximately in equilibrium, therefore the two formulae give similar results. Figures 7 and 8 (Re = 36 000) show that the velocity and turbulent stress profiles calculated with the GI $k - \varepsilon$ model show a good overall agreement with the measurement data, similar to the $k - \omega$ SST model. In the boundary layer before the step ($x/H = -4$), the results of the $k - \omega$ SST model are in perfect agreement with the measurement results, while the GI $k - \varepsilon$ model produces a slightly thicker boundary layer with stronger turbulence. The GI $k - \varepsilon$ model, however, more accurately produces velocity profiles near the wall in the $x/H = 6$ and $x/H = 10$ sections – which defines the boundary layer reattachment length – as well as peak turbulent stresses in the first two sections after the step.

4. CONCLUSION

Although the Kolmogorov flow has been known for more than 70 years and has beneficial properties for the development of turbulence models, it has not been widely used in such areas. Several known Reynolds-averaged turbulence models (e.g., standard $k - \varepsilon$, RNG $k - \varepsilon$, standard $k - \omega$, $k - \omega$ SST, GEKO) lead to qualitatively incorrect results for Kolmogorov flow. The numerical solution leads to increasing turbulent length scale and decreasing flow velocity at nearly constant Reynolds stress. In the current study, it was proposed to eliminate this anomaly by modifying the eddy viscosity formula used in the turbulence model.

The maximum wavelength of the turbulent structures, that can be interpreted in a given model domain, is limited by the size of the domain and the distance from walls. These are taken into account in the models under study by a generalized Δ geometric filter size. The proposed GI eddy viscosity model approximates the eddy viscosity in the dissipation domain by a power function proportional to the square root of the filter size. The dependence of the model on the filter size makes it suitable for avoiding turbulent inflation in Kolmogorov flow.

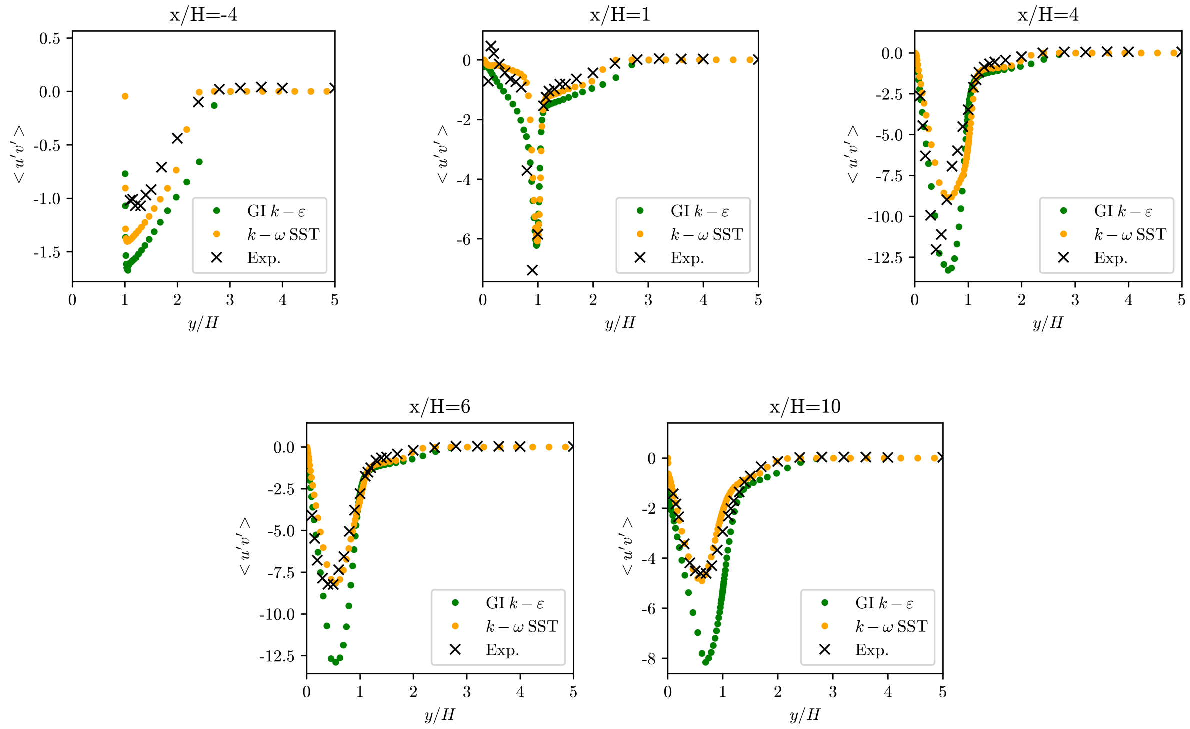

Figure 8. Principal Reynolds stresses calculated from the GI $k-\varepsilon$ model (blue) compared to $k-\omega$ SST model results (orange) and measurement data (black) in flow over a BFS along different x/H profiles.

The GI eddy viscosity model was tested in-situ coupled to the standard $k-\varepsilon$ transport equation in three different flows. In the transport equation of ε, $C_{1\varepsilon}$ was modified from the standard 1.44 to 1.55, to better fit the steady-state channel flow. All other model constants were chosen based on the standard $k-\varepsilon$ model. The resulting GI $k-\varepsilon$ model at $\mathrm{Re}_\Delta = 1000$ channel flow showed excellent agreement with the DNS data and reproduced the peak turbulent kinetic energy near the wall more accurately than the $k-\omega$ SST model.

In Kolmogorov flow, the GI $k-\varepsilon$ model did not exhibit the turbulent inflation typical of known RANS models, but the model produced velocity amplitudes significantly lower than the DNS results. From the DNS analysis of the Kolmogorov flow it was found that the transport equation of ε is consistent with the DNS data when the parameter $C_{1\varepsilon}$ is close to the parameter $C_{2\varepsilon}$. With $C_{1\varepsilon} = C_{2\varepsilon}$ the GI $k-\varepsilon$ model produced results close to the DNS results.

In the high Reynolds number (Re = 36 000) flow above the BFS, the GI $k-\varepsilon$ model showed similar agreement with the $k-\omega$ SST model. A more accurate agreement with the measurement data was observed for the length of the separation bubble.

The further validation of the GI $k-\varepsilon$ model, the addition of Kolmogorov flows excited by time-varying driving force to the DNS database, and the search for models to describe equilibrium shear flow are the planned future directions of the current research.

ACKNOWLEDGEMENT

Project no. TKP-6-6/PALY-2021 has been implemented with the support provided by the Ministry of Culture and Innovation of Hungary from the National Research, Development and Innovation Fund, financed under the TKP2021-NVA funding scheme.

The research reported in this paper is part of project no. **146158**, implemented with the support provided by the Ministry of Innovation and Technology of Hungary from the National Research, Development and Innovation Fund, financed under the **OTKA K 23** funding scheme.

Supported by the **EKÖP-24-3-BME-194** University Research Scholarship Program of the Ministry for Culture and Innovation from the source of the National Research, Development, and Innovation Fund.

REFERENCES

[1] Jones, W. P., and Launder, B. E., 1972, "The prediction of laminarization with a two-equation model of turbulence", *International journal of heat and mass transfer*, Vol. 15 (2), pp. 301–314.

[2] Chou, P.-Y., 1945, "On velocity correlations and the solutions of the equations of turbulent fluctuation", *Quarterly of applied mathematics*, Vol. 3 (1), pp. 38–54.

[3] Menter, F. R., 1994, "Two-equation eddy-viscosity turbulence models for engineering applications", *AIAA journal*, Vol. 32 (8), pp. 1598–1605.

[4] Shih, T.-H., Liou, W. W., Shabbir, A., Yang, Z., and Zhu, J., 1995, “A new k-ε eddy viscosity model for high reynolds number turbulent flows”, *Computers and fluids*, Vol. 24 (3), pp. 227–238.

[5] Ansys Fluent Documentation, “Realizable k-ε Model”, URL https://www.afs.enea.it/project/neptunius/docs/fluent/html/th/node60.htm.

[6] Johns Hopkins Turbulence Database, “Channel Flow Simulation Data”, URL https://turbulence.pha.jhu.edu/Channel_Flow.aspx.

[7] Driver, D. M., and Seegmiller, H. L., 1985, “Features of a reattaching turbulent shear layer in divergent channel flow”, *AIAA journal*, Vol. 23 (2), pp. 163–171.